Kristina KILIKEVIČIENĖ
Jonas MATIJOŠIUS
Antanas FURSENKO
Artūras KILIKEVIČIUS

# TESTS OF HAIL SIMULATION AND RESEARCH OF THE RESULTING IMPACT ON THE STRUCTURAL RELIABILITY OF SOLAR CELLS

## BADANIA SYMULACYJNE WPŁYWU OPADÓW GRADU NA NIEZAWODNOŚĆ KONSTRUKCJI OGNIW SŁONECZNYCH

*The mandatory tests of resistance to hail is carried out in order to qualify solar cell modules according to standards (IEC 61215 and IEC 61646). The efficiency of modern photovoltaic systems decreases significantly, when the crystalline structure of solar cells is damaged as a result of climatic factors, such as wind, hail, etc., which are similar to mechanical-dynamic effects. This work presents a conducted research of efficiency and reliability of solar cells, simulating hail effects. A testbed was created specifically for carrying out experimental research. During the research, solar elements were exposed to impact, cyclic dynamic loads, with the frequency of revolutions of the balls simulating hail ranging from 5 to 20 Hz, the amplitude of the impact excitation acceleration of the solar cell - up to 986 m / s2 and the force amplitude - up to 1129 N. Experimental research results revealed the reliability of photovoltaic modules of different sizes during the simulation of hail. The proposed assessment methodology of hail effects can be successfully applied in studies of the influence of mechanical-dynamic effects of solar cells of different structures.*

*Keywords*: *solar cells, degradation, measurement of mechanical stress, reliability, hail simulation.*

*Przy kwalifikacji modułów ogniw słonecznych do użytkowania przeprowadza się obowiązkowe badania odporności na gradobicie zgodnie z normami IEC 61215 i IEC 61646. Wydajność nowoczesnych systemów fotowoltaicznych znacznie spada, gdy struktura krystaliczna ogniw słonecznych ulega uszkodzeniu w wyniku czynników klimatycznych, takich jak wiatr, gradobicie itp., które przypominają w swoim działaniu obciążenia mechaniczno-dynamiczne. W pracy przedstawiono wyniki badań symulacyjnych wpływu gradobicia na wydajność i niezawodność ogniw słonecznych. Badania prowadzono na specjalnie do tego celu skonstruowanym stanowisku testowym. Podczas badań, elementy słoneczne były wystawiane na cykliczne obciążenia dynamiczne wywoływane uderzeniami kulek symulujących grad o częstotliwości obrotów od 5 do 20 Hz przy amplitudzie przyspieszenia wzbudzenia uderzeniowego ogniwa słonecznego wynoszącej do 986 m/s2 oraz amplitudzie siły do 1129 N. Wyniki symulacji pozwoliły ocenić niezawodność modułów fotowoltaicznych o różnych rozmiarach. Proponowaną metodologię oceny wpływu opadów gradu można z powodzeniem stosować w badaniach oddziaływania obciążeń mechaniczno-dynamicznych na ogniwa słoneczne o różnych strukturach.*

*Słowa kluczowe*: *ogniwa słoneczne, degradacja, pomiar naprężenia mechanicznego, niezawodność, symulacja opadów gradu.*

## 1. Introduction

Changes in weather conditions, such as the impact of hail or effects of severe snow loads, can lead to glass cracks on PV modules, thus damaging them. Such extreme weather conditions (severe hail effects and high snow loads) can destroy modules that cause glass damage due to mechanical impacts, also unveiling hidden damage, because internal solar cell tears and cracks can form along with thermo-mechanical stresses caused by wind and temperature changes, leading to energy losses and negative loss of stiffness of the structure.

Not only industrialists, but also private users use solar energy today, because the price of solar cells has been decreasing due to improving technology and mass production [12, 18]. House roofs and walls are covered in solar cells [2]. Efficiency is a very important indicator for photovoltaic systems [15], while weather conditions decrease the efficiency of solar cells.

Such factors as wind and temperature fluctuations are very important in assessing the longevity and performance efficiency of a particular solar cell and the entire system [5, 8, 14, 16, 17]. Dynami-

mechanical loads result in micro-cracks, which damage the crystal structure of photovoltaic modules [18], which adversely affects the efficiency of light energy conversion and the quality of work of the solar module [3, 4, 9, 20]. In order to reduce the loss of efficiency, knowing the impact of weather conditions is necessary [13, 14], and environmental vibration tests perfectly serve this purpose [6]. Environmental vibration tests are dynamic tests, when the wake-up occurs naturally, for example, from the air flow caused by oscillations of the earth, transport-driven excitation and the like. Excitation forces are not measurable, measuring the response of the experimental object instead. Time and amplitude dependence algorithms have been composed on the basis of the information received [7, 11, 21]. The source of excitation may be wind, periodic or accidental seismic effects or other sources [1].

The performance of the hail test requires expensive space-consuming equipment, which is often difficult to implement. Thus one of the main objectives of this work is to present a simple methodology to simulate hail. The proposed methodology for the assessment

of hail effects can be successfully applied in studying the influence of mechanical-dynamic effects of solar cells of different structures.

## 2. Research object and testbed

The object of research is a photovoltaic (polycrystalline) solar cell, the geometric parameters and other data of which are presented in Table 1.

*Table 1. Photovoltaic (polycrystalline) module solet*

| Specifications | |
|---|---|
| Cell size | 37x156 mm |
| Number of cells | 5x2 |
| Front side glass | 3,2 mm hardened solar glass |
| Dimensions (L x W) | 322 x 204 mm |

A testbed, the main element of which is a motor with a frequency convertor and balls simulating ice cubes, was created for hail simulation. The main purpose of the testbed was to reach the average speed of ice cubes during hail (with the diameter of the cube being 40 mm and its mass – 30 g).

The danger level posed by hail is classified according to the energy of the impact of hail cubes. Kinetic energy generated by a hail cube depends on the mass and speed of the hail cube before the impact (1):

$$E = 1/2\ m\ v^2 \qquad (1)$$

Where: $E$ kinetic energy [J], $m$ mass of hail cube [kg], $v$ impact speed of hail cube [m/s].

The speed of a hail cube (before the impact) is calculated according to the formula (2):

$$v = r\ 2\ \pi\ f \qquad (2)$$

Where: $r$ – radius (from the axis of revolution to the point of impact), m; $f$ – frequency of revolutions per second, Hz.

Changing the radius r and the frequency of revolutions f was possible during the research. Results of the speed of a hail cube ($v$) and kinetic energy ($E$) when changing the radius and frequency of revolutions are presented in Table 2. The speed of a hail cube ($v$) and kinetic energy ($E$) recommended according to the standard [10] with the hail cube weighing 40 g is 27.5 m/s and 11.1 J, respectively.

*Table 2. Results of the hail cube speed (v) and kinetic energy (E) when changing radius r and frequency of revolutions f*

| Seq. No. | r, m | f, Hz | v, m/s | E, J |
|---|---|---|---|---|
| 1 | 0,2 | 5 | 6,28 | 0,790 |
| 2 | 0,25 | 5 | 7,85 | 1,234 |
| 3 | 0,3 | 5 | 9,42 | 1,777 |
| 4 | 0,35 | 5 | 10,99 | 2,418 |
| 5 | 0,4 | 5 | 12,57 | 3,158 |
| 6 | 0,2 | 10 | 12,57 | 3,158 |
| 7 | 0,25 | 10 | 15,71 | 4,935 |
| 8 | 0,3 | 10 | 18,86 | 7,106 |
| 9 | 0,35 | 10 | 21,99 | 9,672 |
| 10 | 0,4 | 10 | 25,13 | 12,63 |
| 11 | 0,2 | 12 | 15,07 | 4,543 |
| 12 | 0,25 | 12 | 18,84 | 7,099 |
| 13 | 0,3 | 12 | 22,61 | 10,222 |
| 14 | 0,35 | 12 | 26,38 | 13,914 |
| 15 | 0,4 | 12 | 30,14 | 18,173 |
| 16 | 0,2 | 14 | 17,58 | 6,184 |
| 17 | 0,25 | 14 | 21,98 | 9,662 |
| 18 | 0,3 | 14 | 26,38 | 13,914 |
| 19 | 0,35 | 14 | 30,77 | 18,938 |
| 20 | 0,4 | 14 | 35,17 | 24,736 |
| 21 | 0,2 | 16 | 20,10 | 8,0770 |
| 22 | 0,25 | 16 | 25,12 | 12,620 |
| 23 | 0,3 | 16 | 30,14 | 18,173 |
| 24 | 0,35 | 16 | 35,17 | 24,736 |
| 25 | 0,4 | 16 | 40,19 | 32,308 |
| 26 | 0,2 | 20 | 25,12 | 12,62029 |
| 27 | 0,25 | 20 | 31,4 | 19,7192 |
| 28 | 0,3 | 20 | 37,68 | 28,39565 |
| 29 | 0,35 | 20 | 43,96 | 38,64963 |
| 30 | 0,4 | 20 | 50,24 | 50,48115 |
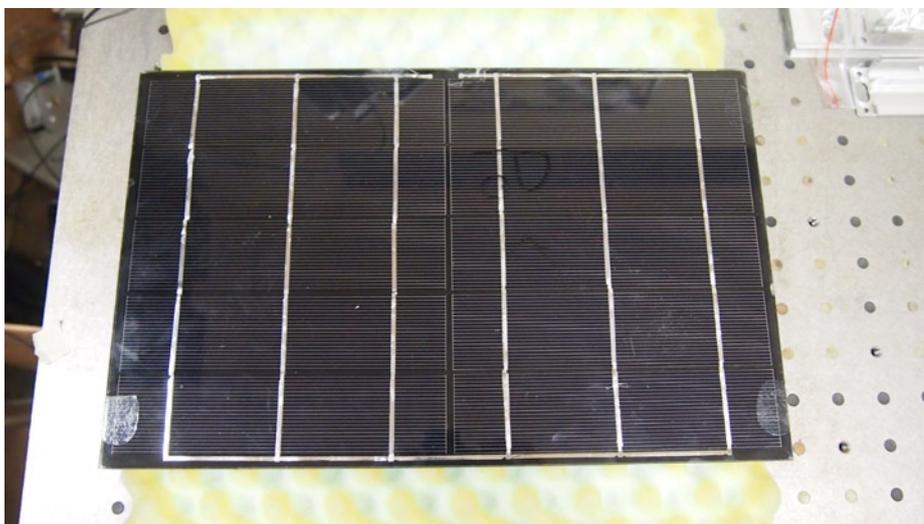


*Fig. 1. General views of solar cells*

The general view of the research solar cells is presented in Fig. 1.

A testbed was used for experimental simulation of actual hail weather conditions. The change of the impact amplitude and frequency of oscillations allows simulating dynamic-mechanical loads that are typical of hail. During the experiments, an accelerometer and a force transducer were attached to the middle of the solar cells.

Fig. 2 presents the general view of the experimental hail simulation testbed (a) and points of attachment of the accelerometer and the force transducer (b). Figure 2a illustrates the part of the testbed simulating hail: a motor Vela STM (position 3) with a frequency convertor Lenze SMVector (position 4); researched solar cell (position 2); data collection and analysis equipment "Machine Diagnostics Toolbox – Type 9727" (position 1); hail simu-
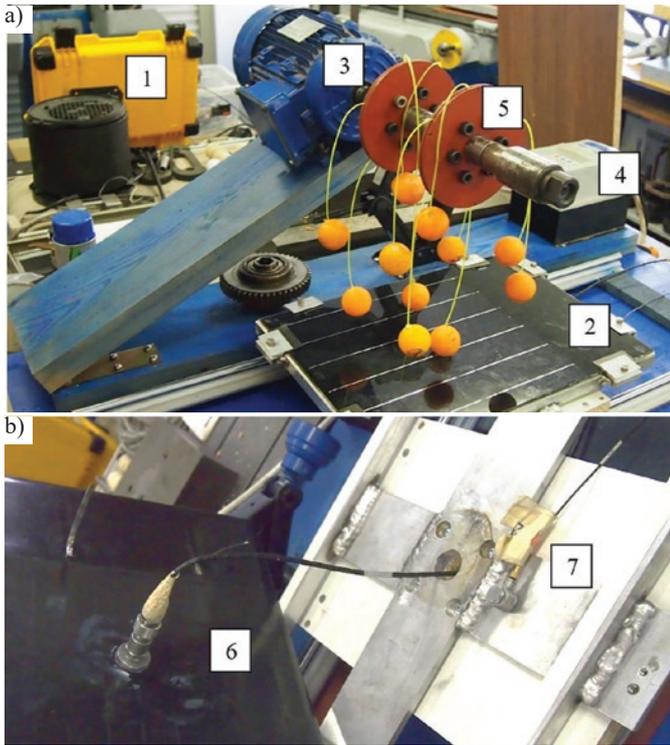
*Fig. 2. (a) general view of the testbed and points of attachment of the accelerometer and the force transducer (b) of the experimental hail simulation testbed*
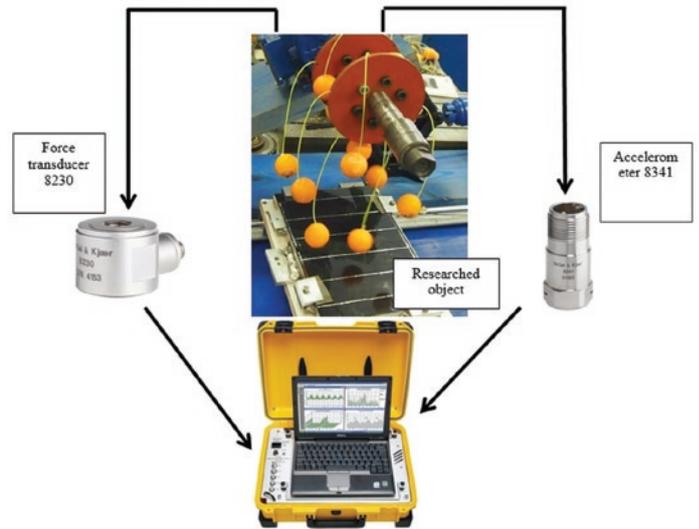


*Fig. 3. Block diagram of the dynamic mechanical load generating facility*

lation cube system (position 5). Figure 2 b illustrates the accelerometer (position 6) and the force transducer (position 7). Sensors were inspected using the best combination: small mass, small dimensions and high sensitivity (of acceleration: Piezoelectric Accelerometer Types 8341 (Voltage Sensitivity 100 mV/g; Amplitude Response 0.5 to 10000 Hz); Force Transducer Types 8230-002 (Voltage Sensitivity 2,2 mV/N).

Block diagram of the testbed is presented in Fig. 3.
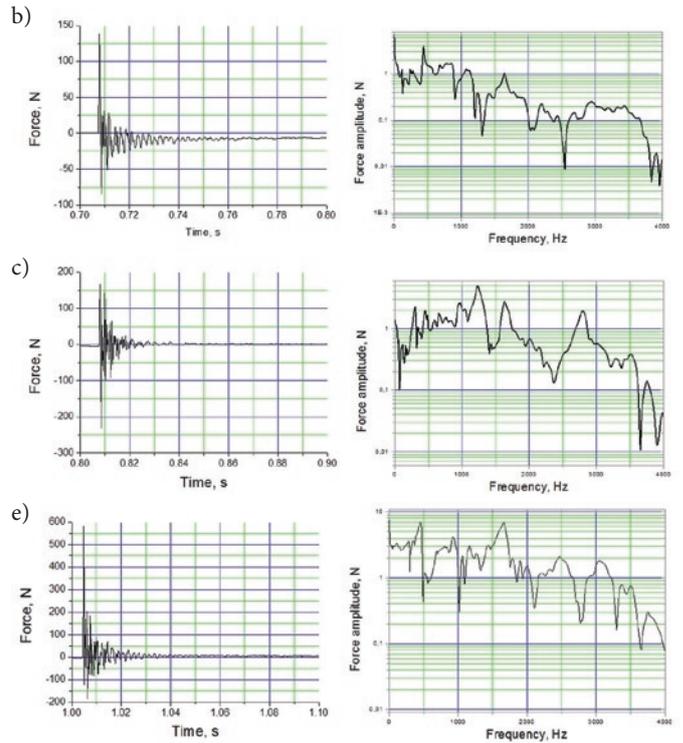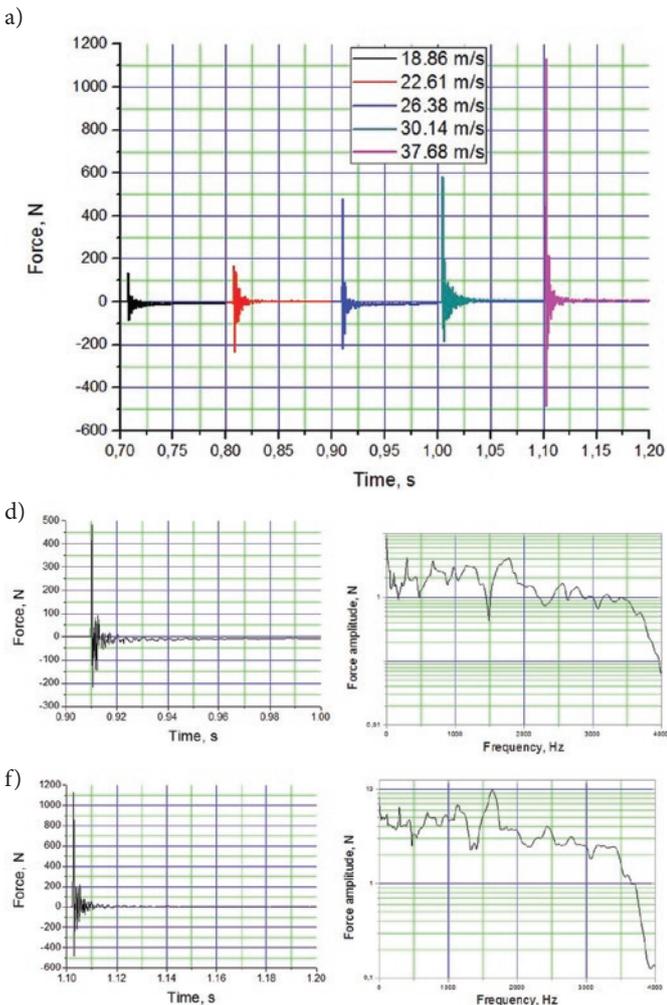


*Fig. 4.  Temporal and spectral density graphs of the vertical direction force of the solar cell midpoint in presence of one impact excitation: a – temporal excitation force graphs (at the linear ball speed v (18.86, 22.61, 26.38, 30.14 and 37.68 m/s)); b – temporal graphs of excitation force and its spectral density at the linear ball speed of 18.86 m/s; c –temporal graphs of excitation force and its spectral density at the linear ball speed of 22.61 m/s; d – temporal graphs of excitation force and its spectral density at the linear ball speed of 26.38 m/s; e – temporal graphs of excitation force and its spectral density at the linear ball speed of 30.14 m/s; f – temporal graphs of excitation force and its spectral density at the linear ball speed of 37.68 m/s*

During the experiment, a cyclic mechanical load was applied when the frequency of revolutions of balls simulating hail ranged from 5 to 20 Hz, the amplitude of the impact excitation acceleration of the solar cell was up to 986 m /s² and the force amplitude - up to 1129 N. Such changes in parameters were sufficient to simulate hail conditions. The equipment used allows determining dynamic parameters of the researched object, which should be evaluated at the time of design and operation of solar cells. This would allow reducing the formation of micro-cracks in the crystalline structure of the solar cell.

## 3. Research results and discussions

The experiment was carried out simulating the impact of hail. The mechanical-dynamic effect was measured (excitation force and acceleration). The maximum amplitudes of excitation force are illustrated in Fig. 4, which presents the results of the measurement of the solar cell midpoint. Fig. 4 presents temporary force graphs and graphs of spectral density of force. The maximum received acceleration amplitudes are presented in Figure 5. Figure 5 illustrates temporal acceleration graphs and graphs of their spectral density. During the experiment, the radius r (from the axis of rotation to the point of impact)

was 0.3 m, changing the linear speed of the ball $v$ (18.86, 22.61, 26.38, 30.14 and 37.68 m / s).

Statistical parameters of the results of measurement of force and acceleration illustrated in Figures 4 and 5 are presented in Table 3.

Data presented in Figures 4 and 5 and Table 3 show experimental measurement results of the impact excitation force and response of the solar cell midpoint acceleration. The assessment of changes in the impact excitation force (Figure 4) at different speeds reveals that the increase in speed every 3.76 m/s (from 18.86 to 30.14 m/s) increases force values (by 20 % comparing the maximum values 137.927 and 166,073 N; 290 % comparing the maximum values 166,073 and 480,814 N; 21 % comparing the maximum values 480,814 and 582,064 N). Speed increase from 30.14 to 37.68 m/s increases force values by

a)



b)



c)



d)



e)
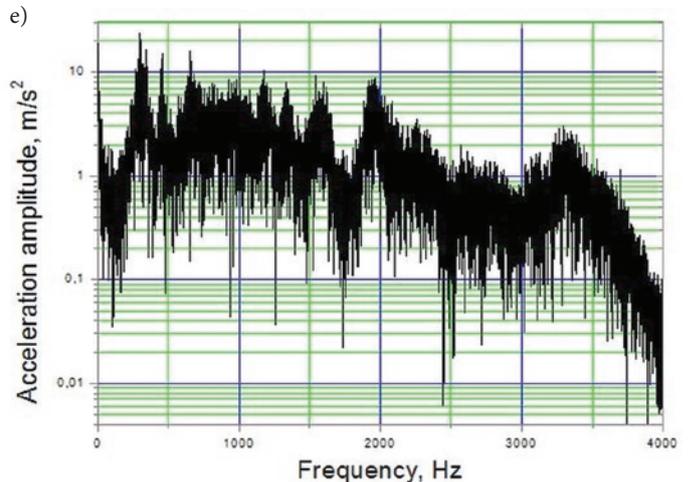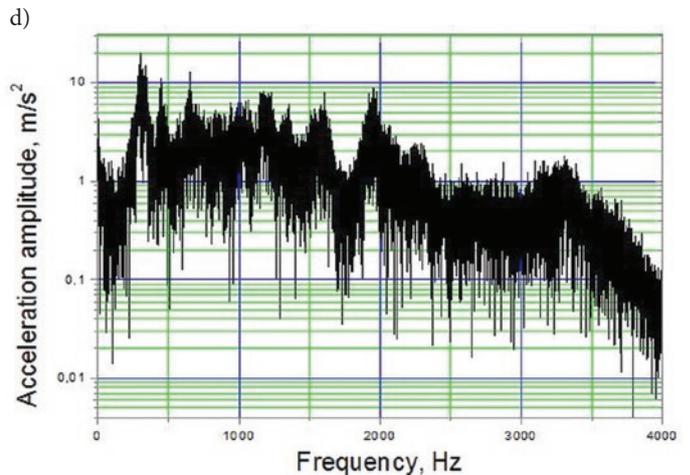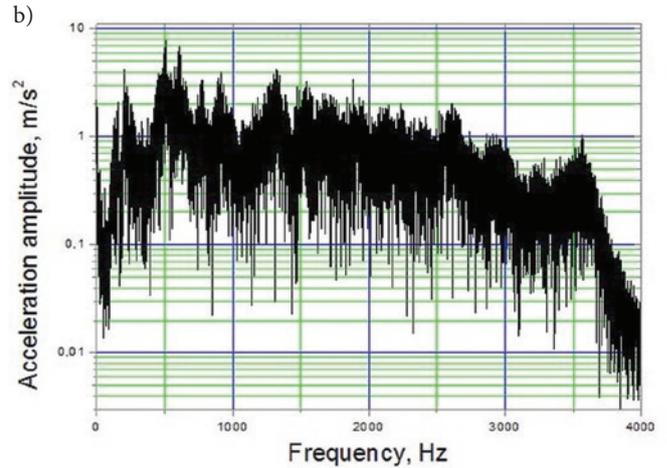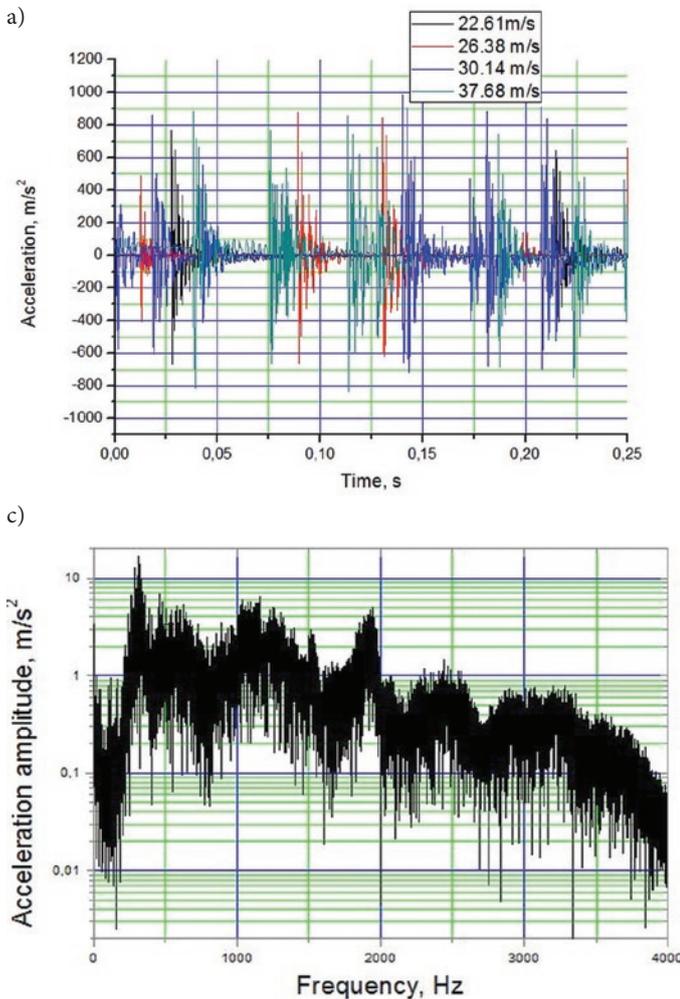


Fig. 5. Temporal and spectral density graphs of the vertical direction force of the solar cell midpoint in presence of hail simulation: a – temporal acceleration graphs (at the linear ball speed v (22.61, 26.38, 30.14 and 37.68 m/s)); b – acceleration spectral density graphs at the linear ball speed of 22.61 m/s; c – acceleration spectral density graphs at the linear ball speed of 26.38 m/s; d – acceleration spectral density graphs at the linear ball speed of 30.14 m/s; e – acceleration spectral density graphs at the linear ball speed of 37.68 m/s

*Table 3. Statistical parameters of the results of measurement of excitation force and acceleration*

| Linear speed v, m/s | Excitation force, N | | |
|---|---|---|---|
| | Standard Deviation | Minimum | Maximum |
| 18.86 | 10,425 | -84,536 | 137,927 |
| 22.61 | 17,795 | -231,507 | 166,073 |
| 26.38 | 25,816 | -216,714 | 480,814 |
| 30.14 | 32,211 | -184,353 | 582,064 |
| 37.68 | 54,633 | -483,972 | 1128,91 |
| | Acceleration, m/s$^2$ | | |
| 22.61 | 63,686 | -781,358 | 832,698 |
| 26.38 | 78,589 | -675,184 | 944,293 |
| 30.14 | 132,255 | -729,196 | 986,152 |
| 37.68 | 156,956 | -877,289 | 977,222 |

a)                                    b)
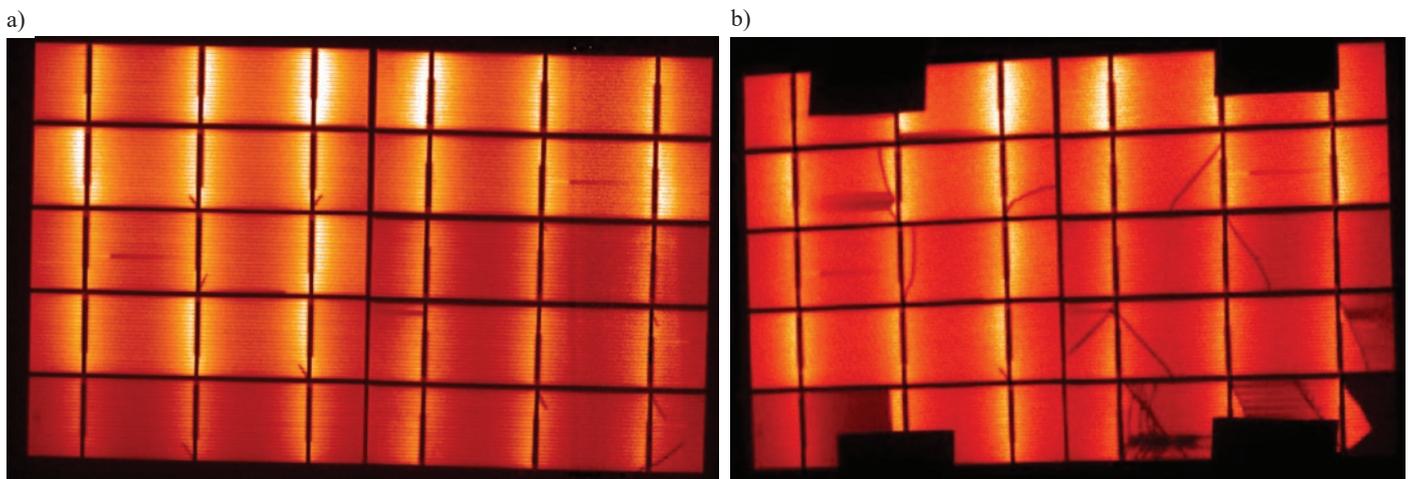


*Fig. 6. Images of solar cells (a – before external effects; b – after external effects)*

a)                                    b)
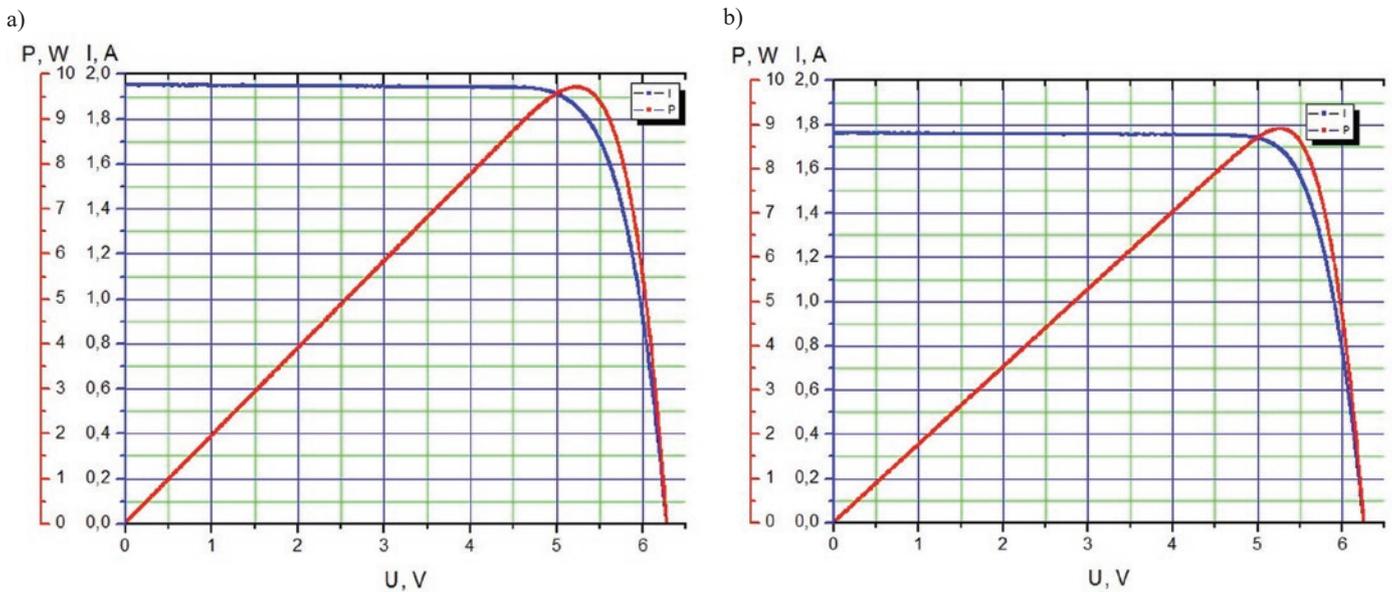


*Fig. 7. Solar cell (from Figure 6) current and power curves (Current I(A); Power (W)) (a – before external effects; b – after external effects)*

194 % comparing the maximum values 582,064 and 1128,91 N. In the assessment of standard deviation values of the solar cell midpoint response, the increase in speed from 22.61 to 26.38 m/s increases acceleration values by 23.4 % comparing the maximum values 63.686 and 78.589 m/s$^2$; respectively, the increase of speed from 26.38 to 30.14 m/s increases acceleration values by 68,3 % comparing the maximum values 78,589 and 132,255 m/s$^2$; respectively, the increase of speed

from 30.14 to 37.68 m/s increases acceleration values by 68.3 % comparing the maximum values 132,255 and 156,956 m/s$^2$.

Fig. 6 presents images of a photovoltaic module before and after hail simulation. It shows limitation use of solar elements in different areas of use for example in new solar panel for the air condition systems in new vehicles [22] etc.

Fig. 7 presents results of measurement of power of the solar cell.

As per Fig. 6 and 7, cracks formed in the crystalline structure of solar cells after dynamic-mechanical loads. Such defects may lead to minor failures in the solar cell energy current or, in the worst case scenario, the solar cell may not function at all. The similar results are presented in the another author's researches [23,24].

In the course of the experimental research, power before and after the external oscillation excitation effects was measured. The average power of the examined solar cell (6 pcs. were evaluated) before hail

simulation was 9.8 W, and power after hail simulation was 8.8 W. The power decreased by about 11.2 %.

## 4. Conclusion

The use of the special testbed, which ensured the creation of mechanical-dynamic loads equivalent to hail conditions, allowed conducting a test of dynamic excitation of the solar cell. The advantage of the testbed is the fact that impact excitation is performed at an angle, which is close to actual hail conditions, because usually the operated elements are affixed at an angle.

Having carried out the hail simulation test, large damage was done to the researched solar cells, which manifested by cracks formed in the crystalline structure and a significant power loss by about 11.2 %.

## References

1.  Anders C, Urbassek H M. Solar wind ion impacts into ice surfaces: A molecular-dynamics study using the REAX force field. Icarus 2017; 282: 351–362, https://doi.org/10.1016/j.icarus.2016.09.037.
2.  Atkinson C, Sansom C L, Almond H J, Shaw C P. Coatings for concentrating solar systems – A review. Renewable and Sustainable Energy Reviews 2015; 45: 113–122, https://doi.org/10.1016/j.rser.2015.01.015.
3.  Du B, Yang R, He Y, Wang F, Huang S. Nondestructive inspection, testing and evaluation for Si-based, thin film and multi-junction solar cells: An overview. Renewable and Sustainable Energy Reviews 2017; 78: 1117–1151, https://doi.org/10.1016/j.rser.2017.05.017.
4.  El Mghouchi Y, Chham E, Krikiz M S, Ajzoul T, El Bouardi A. On the prediction of the daily global solar radiation intensity on south-facing plane surfaces inclined at varying angles. Energy Conversion and Management 2016; 120: 397–411, https://doi.org/10.1016/j.enconman.2016.05.005.
5.  Guo B, Javed W, Pett C, Wu C-Y, Scheffe J R. Electrodynamic dust shield performance under simulated operating conditions for solar energy applications. Solar Energy Materials and Solar Cells 2018; 185: 80–85, https://doi.org/10.1016/j.solmat.2018.05.021.
6.  Gunduz H, Jayaweera D. Reliability assessment of a power system with cyber-physical interactive operation of photovoltaic systems. International Journal of Electrical Power & Energy Systems 2018; 101: 371–384, https://doi.org/10.1016/j.ijepes.2018.04.001.
7.  Hills J M, Michalena E. Renewable energy pioneers are threatened by EU policy reform. Renewable Energy 2017; 108: 26–36, https://doi.org/10.1016/j.renene.2017.02.042.
8.  Kilikevičius A, Čereška A, Kilikevičienė K. Analysis of external dynamic loads influence to photovoltaic module structural performance. Engineering Failure Analysis 2016; 66: 445–454, https://doi.org/10.1016/j.engfailanal.2016.04.031.
9.  Kulesza G, Panek P, Zięba P. Time efficient texturization of multicrystalline silicon in the HF/HNO3 solutions and its effect on optoelectronic parameters of solar cells. Archives of Civil and Mechanical Engineering 2014; 14(4): 595–601, https://doi.org/10.1016/j.acme.2014.02.007.
10. Martins A C, Chapuis V, Virtuani A, Li H-Y, Perret-Aebi L-E, Ballif C. Thermo-mechanical stability of lightweight glass-free photovoltaic modules based on a composite substrate. Solar Energy Materials and Solar Cells 2018; 187: 82–90, https://doi.org/10.1016/j.solmat.2018.07.015.
11. Picotti G, Borghesani P, Cholette M E, Manzolini G. Soiling of solar collectors – Modelling approaches for airborne dust and its interactions with surfaces. Renewable and Sustainable Energy Reviews 2018; 81: 2343–2357, https://doi.org/10.1016/j.rser.2017.06.043.
12. Polimeno M R, Roselli I, Luprano V A M, Mongelli M, Tatì A, De Canio G. A non-destructive testing methodology for damage assessment of reinforced concrete buildings after seismic events. Engineering Structures 2018; 163: 122–136, https://doi.org/10.1016/j.engstruct.2018.02.053.
13. Popoola I K, Gondal M A, Qahtan T F. Recent progress in flexible perovskite solar cells: Materials, mechanical tolerance and stability. Renewable and Sustainable Energy Reviews 2018; 82: 3127–3151, https://doi.org/10.1016/j.rser.2017.10.028.
14. Punge H J, Kunz M. Hail observations and hailstorm characteristics in Europe: A review. Atmospheric Research 2016; 176–177: 159–184, https://doi.org/10.1016/j.atmosres.2016.02.012.
15. Reshma Gopi R, Sreejith S. Converter topologies in photovoltaic applications – A review. Renewable and Sustainable Energy Reviews 2018; 94: 1–14, https://doi.org/10.1016/j.rser.2018.05.047.
16. Smyth M, Pugsley A, Hanna G, Zacharopoulos A, Mondol J, Besheer A, et al. Experimental performance characterisation of a Hybrid Photovoltaic/Solar Thermal Façade module compared to a flat Integrated Collector Storage Solar Water Heater module. Renewable Energy [Internet]. 2018 Apr [cited 2018 Oct 26]; Available from: https://linkinghub.elsevier.com/retrieve/pii/S0960148118304245.
17. Sun L, Gu X H, Song P, Di Y. A generalized equivalent temperature model in a time-varying environment. Eksploatacja i Niezawodnosc - Maintenance and Reliability 2017, 19 (3): 432–440, https://doi.org/10.17531/ein.2017.3.14.
18. Stratakis E, Kymakis E. Nanoparticle-based plasmonic organic photovoltaic devices. Materials Today 2013; 16(4): 133–146, https://doi.org/10.1016/j.mattod.2013.04.006.
19. Teotia M, Soni R K. Applications of finite element modelling in failure analysis of laminated glass composites: A review. Engineering Failure Analysis 2018; 94: 412–437, https://doi.org/10.1016/j.engfailanal.2018.08.016.
20. Višniakov N, Kilikevičius A, Novickij J, Grainys A, Novickij V. Low-cost experimental facility for evaluation of the effect of dynamic mechanical loads on photovoltaic modules. Eksploatacja i Niezawodnosc - Maintenance and Reliability 2015; 17(3): 334–337, https://doi.org/10.17531/ein.2015.3.2.

21. Zhang C, Wu J, Long C, Cheng M. Review of Existing Peer-to-Peer Energy Trading Projects. Energy Procedia 2017; 105: 2563–2568, https://doi.org/10.1016/j.egypro.2017.03.737.
22. Setiyo M, Soeparman S, Wahyudi S, Hamidi N. The Alternative Way to Drive the Automobile Air-Conditioning, Improve Performance, and Mitigate the High Temperature: A Literature Overview. Periodica PolytechnicaTransportation Engineering 2018; 46(1): 36-41, https://doi.org/10.3311/PPtr.8892.
23. Trzmiel G. Determination of a mathematical model of the thin-film photovoltaic panel (CIS) based on measurement data. Eksploatacja i Niezawodnosc - Maintenance and Reliability 2017; 19 (4): 516–521, https://doi.org/10.17531/ein.2017.4.4.
24. Smolinski M., Perkowski T.,Mystkowski A., Dragašius E., Eidukynas D., Jastrzebski R P. AMB flywheel integration with photovoltaic system for household purpose – modelling and analysis. Eksploatacja i Niezawodnosc - Maintenance and Reliability 2017; 19 (1): 86–94, https://doi.org/10.17531/ein.2017.1.12.

**Kristina KILIKEVIČIENĖ**
Department of Mechanical and Material Engineering
Faculty of Mechanical Engineering
Vilnius Gediminas Technical University
Basanavičiaus str. 28, LT-03224 Vilnius, Lithuania

**Jonas MATIJOŠIUS**
Department of Automobile Engineering
Faculty of Transport Engineering
Vilnius Gediminas Technical University
Basanavičiaus str. 28, LT-03224 Vilnius, Lithuania

**Antanas FURSENKO**
Department of Mechanical and Material Engineering
Faculty of Mechanical Engineering
Vilnius Gediminas Technical University
Basanavičiaus str. 28, LT-03224 Vilnius, Lithuania
E-mail:

**Artūras KILIKEVIČIUS**
Institute of Mechanical Science
Faculty of Mechanical Engineering
Vilnius Gediminas Technical University
Basanavičiaus str. 28, LT-03224 Vilnius, Lithuania

E-mails: kristina.kilikeviciene@vgtu.lt, jonas.matijosius@vgtu.lt,
antanas.fursenko@vgtu.lt, arturas.kilikevicius@vgtu.lt